View metadata, citation and similar papers at core.ac.uk

brought to you by CORE

provided by Apollo

Transverse magnetic focussing of heavy holes in a (100) GaAs quantum well

This content has been downloaded from IOPscience. Please scroll down to see the full text.

2015 Semicond. Sci. Technol. 30 102001

(http://iopscience.iop.org/0268-1242/30/10/102001)

View the table of contents for this issue, or go to the journal homepage for more

Download details:

IP Address: 93.93.130.44
This content was downloaded on 12/10/2015 at 16:13

Please note that terms and conditions apply.

OPEN ACCESS
IOP Publishing

Fast Track Communications
Semiconductor Science and Technology

Semicond. Sci. Technol. **30** (2015) 102001 (5pp)
doi:10.1088/0268-1242/30/10/102001

Fast Track Communication

Transverse magnetic focussing of heavy holes in a (100) GaAs quantum well

M Rendell[1], O Klochan[1], A Srinivasan[1], I Farrer[2], D A Ritchie[2] and A R Hamilton[1]

[1] School of Physics, University of New South Wales, NSW 2052, Australia
[2] Cavendish Laboratory, University of Cambridge, Cambridge CB3 0HE, UK

E-mail: Alex.Hamilton@unsw.edu.au

Received 20 July 2015, revised 4 August 2015
Accepted for publication 25 August 2015
Published 14 September 2015

Abstract

We perform magnetic focussing of high mobility holes confined in a shallow GaAs/$Al_{0.33}Ga_{0.67}As$ quantum well grown on a (100) GaAs substrate. We observe ballistic focussing of holes over a path length of up to 4.9 μm with a large number of focussing peaks. We show that additional structure on the focussing peaks can be caused by a combination of the finite width of the injector quantum point contact and Shubnikov–de Haas oscillations. These results pave the way to studies of spin-dependent magnetic focussing and spin relaxation lengths in two-dimentional hole systems without complications of crystal anisotropies and anisotropic g-tensors.

Keywords: magnetic focussing, spintronics, spin–orbit, GaAs

(Some figures may appear in colour only in the online journal)

1. Introduction

The control of the electron's spin degree of freedom is central to the development of spin-based electronics, as well for spin-based quantum computation [1–3]. Key to both of these fields is the need to manipulate the electron spins without magnetic fields. This has driven great interest in the spin–orbit interaction, which allows all electrical control of the electron spin in semiconductor heterostructures [4]. Holes in GaAs/$Al_{0.33}Ga_{0.67}As$ heterostructures not only possess an intrinsically strong spin–orbit interaction, and suffer far less from unwanted interactions with nuclear spins in the host semiconductor, but also have unique properties that have no counterpart in electron systems [5–7].

In systems with strong spin–orbit coupling transverse magnetic focussing can be used as a spin filter, allowing direct measurement of the spin polarization due to the spatial separation of different spin species [8–11]. Transverse magnetic focussing requires high mobility two-dimensional (2D) systems, so that particles travel ballistically with no momentum relaxation between the injector and collector. Previous magnetic focussing experiments with 2D hole systems were performed using heterostructures grown on (311)A substrates, where silicon can be used as a p-type dopant and high hole mobilities could be achieved [8, 9, 12]. However the low symmetry of the (311)A crystal introduces unwanted complexities into the hole spin properties, since the holes have anisotropic in-plane g-factors and non-zero off-diagonal elements in the Lande g-tensor [13, 14]. This greatly complicates analysis of the spin polarization due to spin–orbit interaction.

In the present paper we show that it is possible to perform transverse magnetic focussing of 2D holes grown on (100) substrates, where the high crystal symmetry greatly simplifies the hole spin properties. Furthermore the high hole mobility is achieved in a comparatively shallow 2D hole system, and the extremely high mobility allows for ballistic transport over a

Content from this work may be used under the terms of the Creative Commons Attribution 3.0 licence. Any further distribution of this work must maintain attribution to the author(s) and the title of the work, journal citation and DOI.

 © 2015 IOP Publishing Ltd Printed in the UK

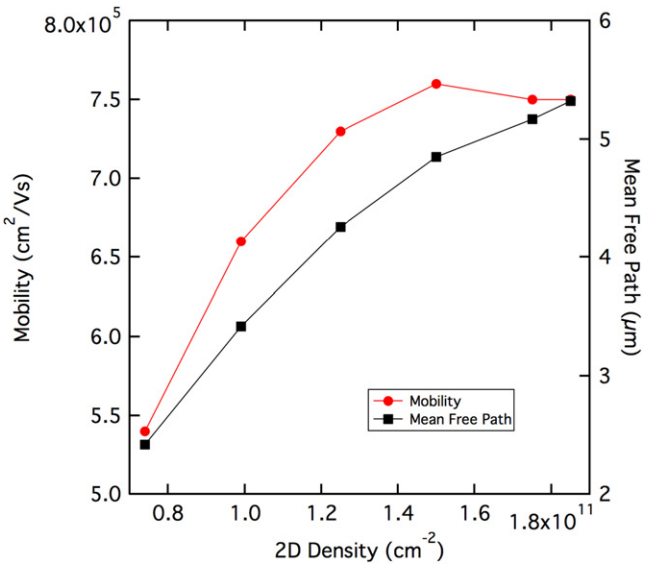

Figure 1. Mobility and mean free path for a range of densities on the 2D Hall bar sample A, measured at the base temperature of 35 mK.

large focussing length, so that magnetic focussing experiments can be performed at very low magnetic fields where the Zeeman spin splitting is negligible.

2. Device characterization

Although high mobility hole systems can be realized on (100) substrates using carbon modulation doping [15–17], making stable p-type nanostructures with Schottky gates is still problematic. We therefore use a completely undoped accumulation mode $Al_{0.33}Ga_{0.67}As/GaAs$ heterostructure containing a 15 nm GaAs quantum well, grown on a (100) substrate (Wafer W713). The holes are introduced into the quantum well by applying a negative bias to an overall top gate [18]. The quantum well confinement lifts the bulk light-hole–heavy hole degeneracy, and in our experiments only the heavy hole band is occupied.

Two samples were used in this study. Sample A is a standard Hall bar used to determine the two-dimensional hole density (p), mobility μ and mean free path (l_{mfp}) as a function of top-gate bias. We calculate the mean free path using the standard equation: $l_{\mathrm{mfp}} = \mu\sqrt{2\pi p}/(e/\hbar)$. Sample B has an additional set of gate electrodes patterned by electron beam lithography, which are used to define three 300 nm wide and 300 nm long quantum point contacts (QPCs) in a magnetic focussing geometry (shown in the inset of figure 2). Experiments were performed in a dilution fridge with a base temperature of 35 mK.

Figure 1 shows the hole mobility and calculated mean free path as a function of density. The high quality of the heterostructure means the holes have the high mobility and long mean free path required to study magnetic focussing. All focussing measurements are performed at a top gate voltage of $V_{\mathrm{TG}} = -1.45$ V, which gives a density of

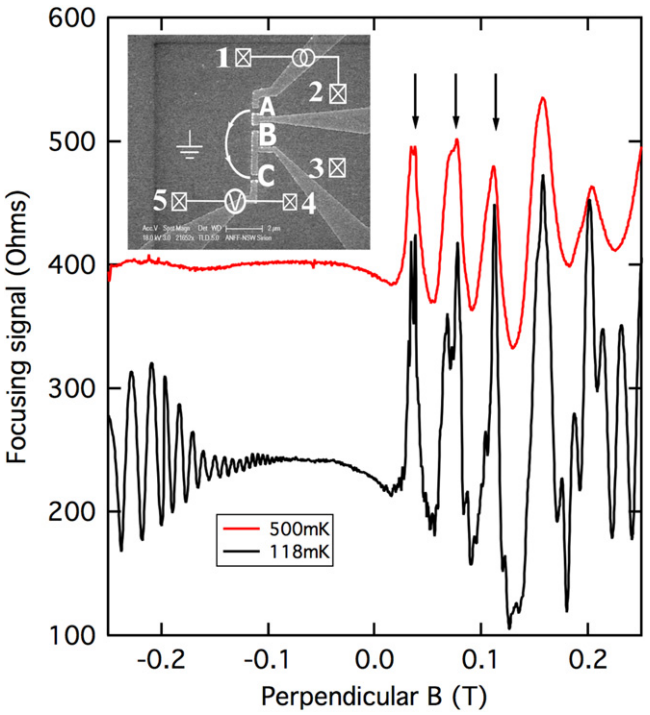

Figure 2. Magnetic focussing of 2D holes at two different temperatures. The inset shows the measurement configuration. A constant current of 5 nA is injected through QPC A using ohmic contacts 1 and 2. The resultant voltage is measured across the detector (QPC C) using contacts 4 and 5, to define a focussing diameter of 3100 nm. The white trace on the schematic diagram shows the path of focussed holes. The focussing resistance is plotted as a function of applied $B_{\perp}$ for both high temperature (top trace) and low temperature (bottom trace). The arrows mark location of focussing peaks predicted by the 2D hole density p_{2D}.

$P_{\mathrm{2D}} = 1.65 \times 10^{11}\,\mathrm{cm}^{-2}$ corresponding to a mobility of 760000 $\mathrm{cm}^2\,\mathrm{V}^{-1}\mathrm{s}^{-1}$ and $l_{\mathrm{mfp}} = 4.9\ \mu$m.

3. Magnetic focussing

The inset of figure 2 shows the gate structure on sample B used to define the focussing geometry. Three QPCs are patterned with separations of 800 nm between QPCs A and B, and 2300 nm between QPCs B and C. This allows for focussing diameters of 800, 2300 and 3100 nm to be used depending on the measurement combination. Five ohmic contacts (labelled 1 to 5) are used to apply a current through the injector QPC and to measure the resulting voltage built up across the collector QPC. The 2D hole reservoir is grounded with a separate ohmic contact to act as a drain for holes that are not received by the collector.

For the data shown in figure 2 the four terminal focussing resistance was measured by injecting a constant current of $I = 5$ nA through QPC A using ohmic contacts 1 and 2. A perpendicular out-of plane magnetic field $B_{\perp}$ was then used to focus the holes into the collector QPC C, with the resulting focussing voltage (V_{focus}) measured between contacts 4 and 5. The gates defining both QPC A and C were symmetrically biased with a voltage of $V_{\mathrm{SG}} = -0.43$ V such that each QPC

was sitting on the first conductance plateau, $G = 2e^2/h$. The resulting focussing resistance ($R_{\text{focus}} = V_{\text{focus}}/I$) is plotted as a function of $B_\perp$ in figure 2.

The top trace in figure 2 shows the magnetic focussing signal at $T = 500$ mK. There is a clear asymmetry in the focussing resistance around $B_\perp = 0$ T. For $B_\perp < 0$ T no focussing peaks or other structure is observed, with clear focussing peaks visible for $B_\perp > 0$ T. The magnetic field at which the first three focussing peaks should occur can be calculated from the 2D hole density: $B_{\text{focus}} = i\hbar k_{\text{F}}/ed$, where $k_{\text{F}} = (2\pi p_{\text{2D}})^{1/2}$, i is an integer and d is the focussing diameter. The expected locations of the first three peaks are marked by vertical arrows in figure 2. There is good agreement between the values predicted from the hole density and the peak locations observed in experiment.

Reducing the temperature to 118 mK causes two changes, shown in the bottom trace of figure 2. Firstly, Shubnikov–de Haas oscillations, periodic in $1/B$, become visible for $B_\perp < -0.1$ T Secondly, for $B_\perp > 0$ additional higher frequency structure appears superimposed on top of the focussing peaks. For $B_\perp < 0.15$ T this structure is periodic in $1/B$ and coincides with the Shubnikov–de Haas oscillations in the 2D region ($B_\perp < 0$), highlighting the need to avoid large magnetic fields in focussing experiments.

In contrast at low fields the additional structure is periodic in B for $B_\perp < 0.15$ T. This high frequency structure is likely an interference effect arising from either the finite width of the injector QPC [19–21], branching flow caused by background impurities [22–24], or some combination of these. To shed some light on to the origins of this high frequency structure, and investigate how the transverse magnetic focussing depends on the focussing distance and the magnetic field, we use the flexible device geometry to examine focussing for different d using different combinations of injector and collector QPCs. Figure 3 shows focussing for all three available focussing diameters, with the inset showing the measurement configuration for each trace. Focussing peaks can be seen for all focussing diameters, ranging from $d = 3100$ nm in figure 3(a) to 800 nm in figure 3(c).

As the focussing length is increased, the location of the focussing peaks shifts to lower $B_\perp$. This is advantageous since it allows the first peaks to occur at low enough $B_\perp$ that there is no unwanted structure caused by Shubnikov–de Haas oscillations. Again higher frequency structure is observed on top of the focussing peaks and troughs, which is rapidly washed out by increasing temperature. This additional structure is periodic in $B_\perp$, with figure 4(c) showing the period in $B_\perp$ of the structure as a function of focussing diameter. The period of the structure decreases linearly as the first peak moves to lower $B_\perp$ (focussing diameter is increased). This is consistent with the structure being caused by the finite width of the injector QPC, which will give self-similar interference patterns for different focussing lengths due to a difference in path length and Aharonov–Bohm phase [19]. This is also consistent with the noticeable broadening of the focussing peaks as the focussing diameter is decreased (figures 3(a)–(c)). Since the injector and collector QPCs have a finite width W_{QPC} (of order the Fermi wavelength) there is a range of

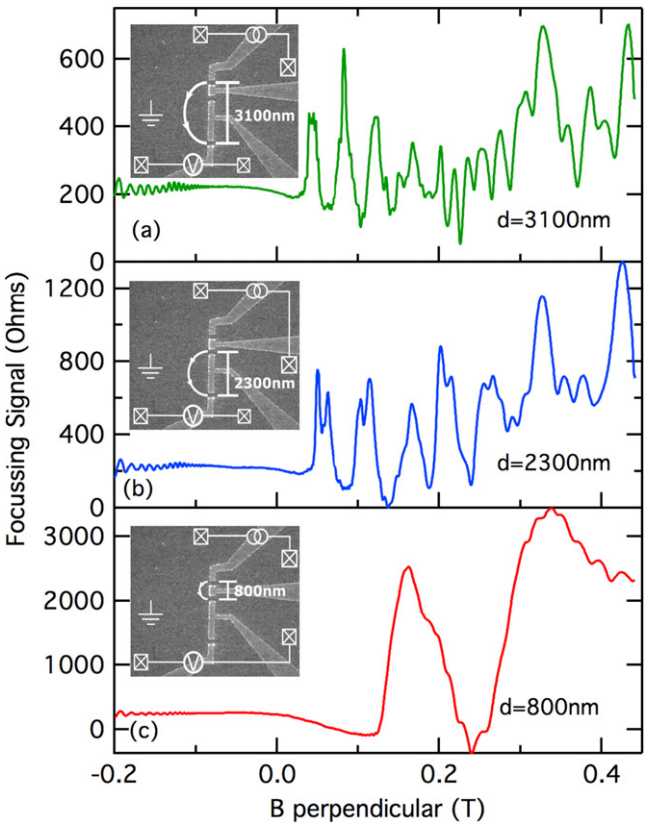

Figure 3. Focussing resistance for different focussing diameters. (a) $d = 3100$ nm, injecting holes from QPC A and collecting in QPC C. (b) $d = 2300$ nm, using QPCs B and C. (c) $d = 800$ nm, using QPCs A and B. All traces were taken with 5 nA injection current at $T = 35$ mK.

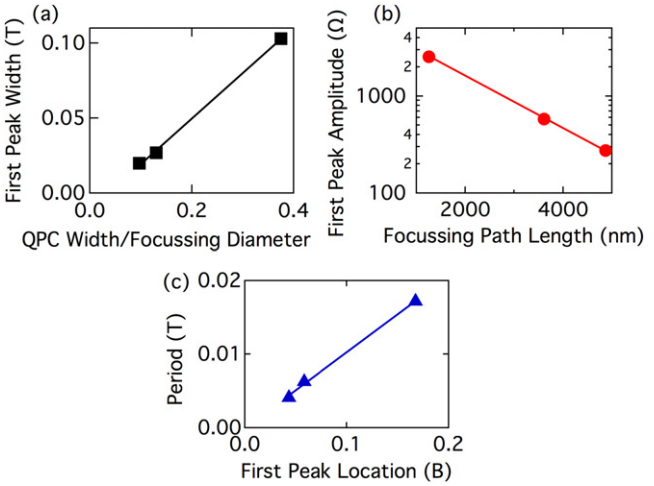

Figure 4. (a) Width of the first focussing peak as a function of the ratio of the QPC width to the focussing diameter. (b) Amplitude of first focussing peak as a function of the focussing path length πd. (c) Period of the high frequency structure as a function of the location of the first focusing peak.

cyclotron orbits, and corresponding $B_\perp$, for which holes will be accepted into the collector QPC. If we assume this broadening of the focussing peaks is approximately $\Delta B_\perp = \hbar k_{\text{F}}/e\Delta d$ where $k_{\text{F}} = (2\pi p_{\text{2D}})^{1/2}$ we expect broader

peaks for smaller d. Figure 4 (a) shows the peak width (ΔB) scales with W_{QPC}/d as expected.

Finally we turn to the amplitude of the focussing peaks. The decrease in the amplitude of the focussing peaks with increasing d is a consequence of the the increased chance of scattering as the focussing path length is increased (figures 3(c)–(a)). This data can be used to extract the scattering length l_0 since $R_{Focus} \propto A \exp(-\pi d/2l_0)$, where $\pi d/2$ is the focussing path length. Figure 4 (b) shows the amplitude of the first focussing peak as a function of the focussing path length $\pi d/2$ on a semilog plot. The exponential decay of the focussing signal gives a scattering length of $l_0 = 1.6\ \mu$m, which is significantly shorter than the momentum relaxation length in the 2D system ($l_\mu = 4.9\ \mu$m). The ratio of these scattering lengths ($l_\mu/l_0 \approx 3.1$) is consistent with values found in previous studies of hole transverse magnetic focussing on (311)A substrates [12], and is likely due to the fact that the momentum relaxation length is not sensitive to small angle scattering, whereas small angle scattering may cause holes to miss the collector QPC. A similar difference in the quantum and momentum scattering times has been observed in accumulation mode electron systems [25].

4. Conclusions

We have shown that high mobility 2D hole systems can be formed on (100) substrates and used to study transverse magnetic focussing over path lengths as large as 4.87 μm. We have shown that additional structure observed at low temperatures arises from the finite with of the injector QPC at low magnetic fields, and Shubnikov–de Haas oscillations at higher magnetic fields. This work paves the way to future studies of spin–orbit driven spin-dependent magnetic focussing and spin relaxation lengths in 2D hole systems without the complications of crystal anisotropies and anisotropic g-tensors.

Acknowledgments

We thank Scott Liles, Samuel Bladwell, Oleg Sushkov and Ulrich Zülicke for numerous discussions. This project was supported by the Australian Research Council (ARC) DP Scheme and the EPSRC (UK). O K acknowledges an ARC DECRA fellowship. Devices were fabricated using facilities at the UNSW Node of Australian National Fabrication Facility (ANFF).

References

[1] Wolf S, Awschalom D, Buhrman R, Daughton J, von Molnár S, Roukes M, Chtchelkanova A and Treger D 2001 Spintronics: a spin-based electronics vision for the future *Science* **294** 1488–95

[2] Awschalom D D and Flatté M E 2007 Challenges for semiconductor spintronics *Nat. Phys.* **3** 153–9

[3] Cerletti V, Coish W A, Gywat O and Loss D 2004 Recipes for spin-based quantum computing *Nanotechnology* **16** R27–49

[4] Datta S and Das B 1990 Electronic analog of the electro-optic modulator *Appl. Phys. Lett.* **56** 665

[5] Keane Z K *et al* 2011 Resistively detected nuclear magnetic resonance in n- and p-type GaAs quantum point contacts *Nano Lett.* **11** 3147–50

[6] Wang L and Wu M W 2012 Hole spin relaxation in p-type (111) GaAs quantum wells *Phys. Rev. B: Condens. Matter Mater. Phys.* **85** 235308

[7] Winkler R 2003 *Spin–Orbit Coupling Effects in Two-Dimensional Electron and Hole Systems* (Berlin: Springer)

[8] Rokhinson L P, Larkina V, Lyanda-Geller Y B, Pfeiffer L N and West K W 2004 Spin separation in cyclotron motion *Phys. Rev. Lett.* **93** 146601

[9] Rokhinson L P, Pfeiffer L N and West K W 2006 Spontaneous spin polarization in quantum point contacts *Phys. Rev. Lett.* **96** 156602

[10] Heremans J J, Chen H, Santos M B, Goel N, van Roy W and Borghs G 2007 Spin-dependent transverse magnetic focusing in InSb- and InAs-based Heterostructures *AIP Conf. Proc.* **893** 1287–8

[11] Rokhinson L P, Pfeiffer L N and West K W 2008 Detection of spin polarization in quantum point contacts *J. Phys.: Condens. Matter* **20** 164212

[12] Heremans J J, Santos M B and Shayegan M 1992 Observation of magnetic focusing in two-dimensional hole systems *Appl. Phys. Lett.* **61** 1652

[13] Winkler R, Papadakis S J, de Poortere E P and Shayegan M 2000 Highly anisotropic g-factor of two-dimensional hole systems *Phys. Rev. Lett.* **85** 4574–7

[14] Yeoh L A, Srinivasan A, Klochan O, Winkler R, Zülicke U, Simmons M Y, Ritchie D A, Pepper M and Hamilton A R 2014 Noncollinear paramagnetism of a GaAs two-dimensional hole system *Phys. Rev. Lett.* **113** 236401

[15] Reuter D, Wieck A D and Fischer A 1999 A compact electron beam evaporator for carbon doping in solid source molecular beam epitaxy *Rev. Sci. Instrum.* **70** 3435–8

[16] Gerl C, Schmult S, Tranitz H-P, Mitzkus C and Wegscheider W 2005 Carbon-doped symmetric GaAsAlGaAs quantum wells with hole mobilities beyond $10^6\ cm^2\ V^{-1}s^{-1}$ *Appl. Phys. Lett.* **86** 252105

[17] Manfra M J, Pfeiffer L N, West K W, de Picciotto R and Baldwin K W 2005 High mobility two-dimensional hole system in gaasalgaas quantum wells grown on (100) gaas substrates *Appl. Phys. Lett.* **86** 252108

[18] Harrell R H, Pyshkin K S, Simmons M Y, Ritchie D, Ford C J B, Jones G and Pepper M 1999 Fabrication of high-quality one- and two-dimensional electron gases in undoped GaAs/AlGaAs heterostructures *Appl. Phys. Lett.* **74** 2328

[19] van Houten H, Beenakker C W J, Williamson J G, Broekaart M E I, van Loosdrecht P H M, van Wees B J, Mooij J E, Foxon C T and Harris J J 1989 Coherent electron focusing with quantum point contacts in a two-dimensional electron gas *Phys. Rev.* B **39** 8556–75

[20] Spector J, Stormer H L, Baldwin K W, Pfeiffer L N and West K W 1990 Electron focusing in two-dimensional systems by means of an electrostatic lens *Appl. Phys. Lett.* **56** 1290–2

[21] Khatua P, Bansal B and Shahar D 2014 Single-slit electron diffraction with Aharonov–Bohm phase: Feynman's thought experiment with quantum point contacts *Phys. Rev. Lett.* **112** 010403

[22] Koonen J J, Buhmann H and Molenkamp L W 1999 Probing the potential landscape inside a two-dimensional electron-gas *Phys. Rev. Lett.* **84** 2473

[23] Topinka M A, LeRoy B J, Westervelt R M, Shaw S E J, Fleischmann R, Heller E J, Maranowski K D and

Gossard A C 2001 Coherent branched flow in a two-dimensional electron gas *Nature* **410** 183–6

[24] Aidala K E, Parrott R E, Kramer T, Heller E J, Westervelt R M, Hanson M P and Gossard A C 2007 Imaging magnetic focusing of coherent electron waves *Nat. Phys.* **3** 464–8

[25] MacLeod S J, Chan K, Martin T P, Hamilton A R, See A, Micolich A P, Aagesen M and Lindelof P E 2009 Role of background impurities in the single-particle relaxation lifetime of a two-dimensional electron gas *Phys. Rev. B.: Condens. Matter Mater. Phys.* **80** 035310